#### **CONFERENCE PRE-PRINT**

# OVERVIEW OF THE PHYSICS DESIGN OF THE EHL-2 SPHERICAL TORUS FOR PROTON-BORON FUSION

H. S. Xie, Y. F. Liang, Y. J. Shi, X. Gu, X. C. Jiang, L. L. Dong, X. Y. Wang, D. K. Yang, W. J. Liu, T. T. Sun, Y. M. Wang, Z. Li, J. Q. Cai, X. M. Song, M. Z. Tan, G. Yang, H. Y. Zhao, J. Q. Dong, Y. K. M. Peng, S. D. Song, Z. Y. Chen, Y. Y. Li, B. Liu, D. Luo, Y. M. Yang, M. S. Liu, and the EHL-2 Team 1Hebei Key Laboratory of Compact Fusion, Langfang, China 2ENN Science and Technology Development Co., Ltd, Langfang, China

Email: xiehuasheng@enn.cn

#### Abstract

ENN Science and Technology Development Co., Ltd. (ENN) is committed to generating fusion energy in an environmentally friendly and cost-effective manner, which requires abundant aneutronic fuel [1]. Proton-boron (p-11B or p-B) fusion is considered an ideal choice for this purpose. Recent studies have suggested that p-B fusion, although challenging, is feasible based on new cross section data, provided that a hot ion mode (Fig 1) and high wall reflection can be achieved to reduce electron radiation loss. The high beta and good confinement of the spherical torus (ST) make it an ideal candidate for p-B fusion. ENN is planning the next experiment EHL-2 (typical parameters shown in Table 1) with the goal to verify the thermal reaction rates of p-11B fusion, establish spherical torus/tokamak (ST) experimental scaling laws at 10's keV temperature, and provide a design basis a succeeding experiment aiming to test and achieve p-11B fusion burn. Here, we give an overview of the physics design of the EHL-2.

### 1. INTRODUCTION

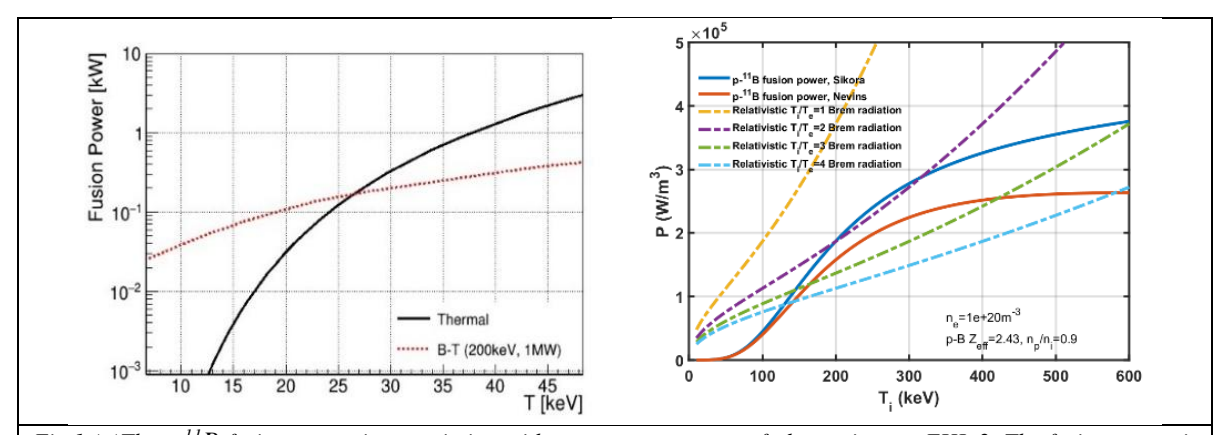


Fig.1 (a)The  $p^{-11}B$  fusion power in association with center temperature of plasma ions at EHL-2. The fusion power is mainly released by thermal (black solid curve) and beam-thermal (B-T) (red dash curve) reactions. The beam is considered as 200keV and 1MW, with a source of hydrogen. (b) Fusion power density produced in  $p^{-11}B$  plasma and bremsstrahlung radiation as a function of the ion temperature[2].

Based on 0-dimential system design and 1.5-dimentional transport modelling analyses, the main target parameters of EHL-2 have been basically determined, including the plasma major radius,  $R_0$ , of 1.05 m, the aspect ratio, A, of 1.85, the maximum central toroidal magnetic field strength,  $B_0$ , of 3 T, and the maximum plasma toroidal current,  $I_p$ , of 3 MA. The main heating system will be the NBI ion heating at a total power of 17 MW. In addition, 6 MW of electron cyclotron resonance heating (ECRH) will serve as the main means of current localization drive and MHD instability control.

The physics design of EHL-2 is focused on addressing three main operating scenarios, i.e., 1) high ion temperature scenario (Fig. 2), 2) high-performance steady-state scenario and 3) high triple product scenario. Each scenario will integrate solutions to different important issues, including equilibrium configuration, heating and current drive, confinement and transport, MHD instability, p-11B fusion reaction, plasma-wall interactions, etc.

Beyond that, there are several unique and significant challenges to address, including:

- establish a plasma with extremely high core ion temperature (T<sub>i,0</sub>>30keV), and ensure a large ion-to-electron temperature ratio (T<sub>i,0</sub>/T<sub>e,0</sub> > 2), and a boron concentration of 10-15% at the plasma core;
- non-inductive current driving the start-up and rise of MA-level toroidal current plasma. This is because the volt-seconds that the central solenoid of the ST can provide are very limited;
- achieve divertor heat and particle fluxes control including complete detachment under high P/R (>20MW/m) at relatively low densities.

Over the past two years, the technology routes and challenges associated with the physics design of the EHL-2 device have been identified and systematically analyzed. Major results are presented in a Special Issue in Plasma Science and Technology [2]. It is worth noting that due to

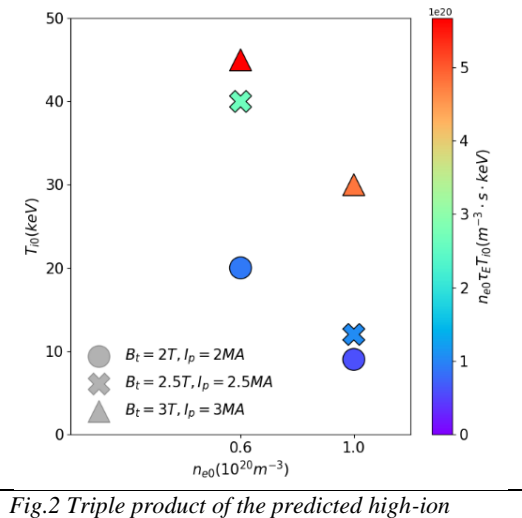


Fig.2 Triple product of the predicted high-ion temperature scenario[2].

the scarcity of spherical torus and p-11B fusion experimental data, the design of devices was heavily reliant on models derived from conventional tokamak experiments, some of which may be inappropriate. This underscores the importance of a robust experimental research program like EHL-2.

Table 1. System code design results of EHL-2 major parameters. The heating power listed is the power absorbed by the plasma[2]

Parameters	EHL-2 (Ver1.0)	EHL-2 (Standard)	EHL-2 (Low)	EHL-2 (Medium)	EHL-2 (High)	EHL-2 (Goal)	
Avg./peak T <sub>i</sub> (keV)	-/30	-/35	-/25	-/34	-/50	-/50	
Avg./peak $n_{\rm e}$ (m <sup>-3</sup> )	$-/1.44 \times 10^{20}$	-/2.22×10 <sup>20</sup>	$-/1.33 \times 10^{20}$	$-1.33 \times 10^{20}$	$-/2.05 \times 10^{20}$	-/1.66×10 <sup>20</sup>	
Confinement time $\tau_{E}(s)$	0.5	0.6	0.3	0.5	2.5	1.2	
Beta $\beta$	11%	11%	10%	14%	14%	21%	
Major radius R	1.05	1.05	1.05	1.05	1.05	1.05	
Aspect ratio A	1.85	1.85	1.85	1.85	1.85	1.85	
Magnetic B	3.0	3.0 6.09	2.0	2.0	3.0	3.0 6.47	
Beta $\beta_{ m N}$	6.17		4.7	6.39	6.35		
Beta $\beta_p$	3.2	3.1	1.9	2.6	2.6	1.8	
Safety factor q	3.83 (5.55*)	3.83 (5.55*)	3.07 (4.45*)	3.07 (4.45*)	3.03 (4.4*)	2.09 (3.03*)	
Density limit $n_{avg}/n_{gw}$	0.4	0.5	0.36	0.36	0.36	0.25	
Heating power $P_{\text{heat}}$ (MW)	19	16	13.5	11	6	16	
Plasma current $I_p$ (MA)	3.0	3.0	2.5	2.5	3.8	5.5	
ST $H$ factor $H_{\rm ST}$	0.657	0.598	0.632	0.94	1.25	0.908	
Comments	$S_{n} = 0.4,$ $S_{T} = 0.8$	Overall best	Engineering & physics low	Engineering low & physics high	Engineering & physics high	*ST $q$ , and $S_n = 0.4$ , $S_T = 0.8$	

This overview will introduce the advanced progress in the physics design of EHL-2.

### 2. PHYSICS DESIGN: MAJOR PARAMETERS AND OPERATING SCENARIOS

Based on the 0-D physics design and weighing the technical difficulty, the top-level device parameters of EHL-2 are basically confirmed. Figure 3 shows the schematic diagram and cross-section of the main magnet system and vacuum vessel structure. The main magnet system consists of 16 D-shaped copper toroidal field (TF) coils (evenly distributed in toroidal direction) and 12 circular copper poloidal field (PF) coils (up-down symmetrical distribution). The maximum toroidal magnetic field at  $R_0 = 1.05$  m can be up to 3 T with a flat-top of about 2.3 s, or 2 T with a flat-top of more than 6 s. The toroidal ripple at the last closed flux surface in the middle-plane at the low field side is very small, and it is below 0.01%. This is mainly because the TF coils are located outside of the PF coils and are far away from the plasma surface.

Due to limited space, the CS will adopt an integrated design, directly wrapped around the TF coil and cannot be segmented. This CS coil can provide up to 5 Vs, which will be mainly used to assist in controlling the plasma

current. The PF coils will be mainly used to control the plasma horizontal and vertical displacements, the plasma shape and the divertor configuration. To reduce the impact on the main plasma shape, the divertor coils PF 5–8 are located a bit farther away from the main plasma. Furthermore, considering the future operation safety and convenient engineering maintenance of the device, all PF coils are placed outside the vacuum vessel (VV). This requires that the VV structure needs a special shape structure in some areas to cater to the layout of the PF coils. But in this way, the plasma is much closer to VV, which is of great help in alleviating the vertical displacement events (VDE) of plasma.

## 2.1 Configuration flexibility

Through multiple engineering iterations, the locations and required current ranges for all 12 PF coils were finally determined. This PF system is capable of achieving a series of double-null divertor equilibrium configurations, including X-point (XPT) configuration, Super-X configuration, and conventional poloidal divertor configuration. For the XPT configuration, the secondary X-point can be actively controlled to move not only away from the divertor target but also from the scraped-off layer (SOL) to the divertor private flux region.

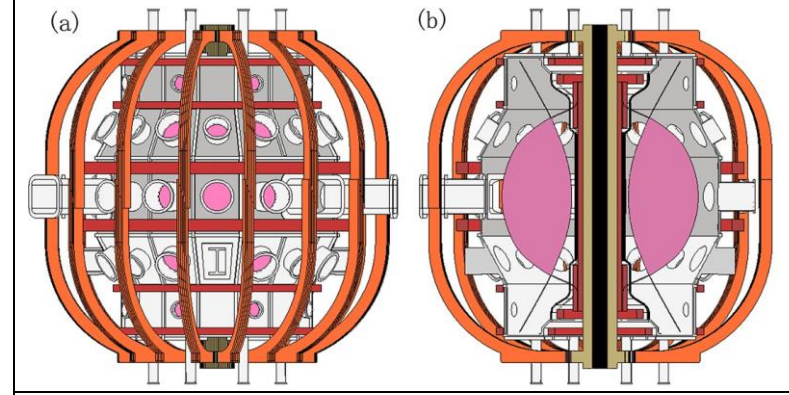


Fig.3 (a) Schematic diagram and (b) cross-sectional view of the main magnet system and vacuum vessel structure[2].

#### 2.2 Heating and current drive

To achieve and maintain the plasma performance of the EHL-2 physics design, various auxiliary heating and current drive (H&CD) systems have been considered as shown in table 2.

Table 2. Design of heating and current drive systems in EHL-2[2]

H&CD system	EHL-2 parameters	Input power (MW)		
	1×4 MW@60 keV/5 s			
NBI	2×5 MW@80–100 keV/5 s	17		
	1×3 MW@200 keV/5 s			
EC	1×1 MW@50 GHz/5 s	7		
	6×1 MW@105&140 GHz/5 s (dual frequency)	,		
IC (Phase II)	5 MW@30–75 MHz/5 s	5		
LHW (Phase II)	2 MW@2.45–5 GHz/5 s	2		

The NBI heating system will provide a total input power of 17 MW, including one negative ion source NBI (N-NBI) with a power and beam energy of 3 MW@200 keV, and two positive ion source NBI (P-NBI) with 10 MW@80–100 keV and 4 MW@60 keV respectively. They all employ tangential injection with the beamlines optimized for energy deposition near the plasma axis. Simulation results show that, within the range of plasma parameters designed for EHL-2, all of these beams preferentially heat ions rather than electrons. It should be noted that the N-NBI can be used not only for heating and current drive, but also for p-11B beam target fusion reaction research.

EHL-2 will be equipped with two ECRH systems. One is a 50 GHz system with a power of 1 MW, which will be used for plasma start-up and auxiliary current ramp-up. Another is a 105/140 GHz dual-frequency system with a power of 6 MW, which will be used to control the plasma current density profile and mitigate MHD instabilities. Here, the selection of these two frequencies is based not only on the available frequency window under the toroidal magnetic field strength of the equipment design, but also on the current drive efficiency at low and high plasma densities.

### 2.3 The framework of ENN integrated modelling

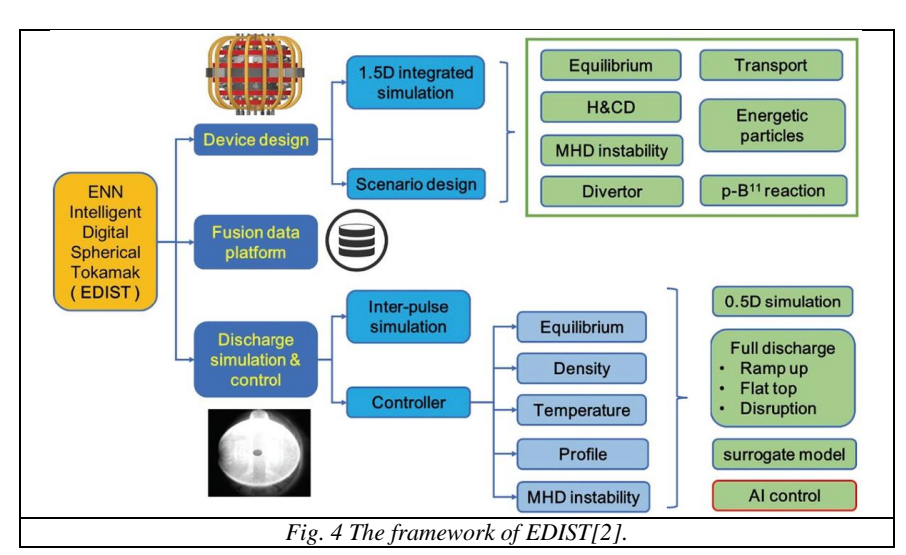
In support of EHL-2 physics design and future experimental operations, the ENN Digital Intelligent Spherical Torus project (EDIST) has been under development since 2023. This project aims to build a platform for numerical modelling and future artificial intelligent (AI) applications in ST devices. Figure 4 shows the framework of EDIST.

Besides the fusion data platform, two major branches of its applications have been organized. One branch of EDIST focuses on developing tools for device design, primarily based on 1.5-D, which are further applied to design operational scenario of the device. Another branch of EDIST focuses on developing tools for discharge, with the purpose of supporting simulation and control. AI control of plasma will be one of the most important directions in this area.

# 2.4 Operating scenarios

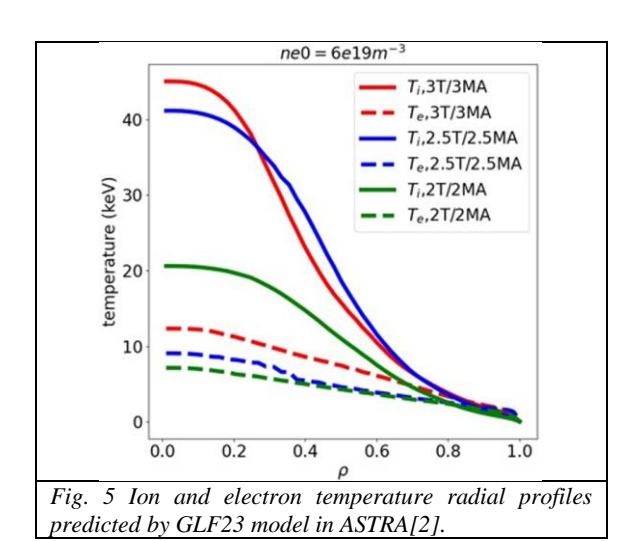
# 2.4.1 High ion temperature scenario

To evaluate the feasibility of 0-D design parameters of high-ion-temperature scenario, core transport analysis is conducted via fluid simulations based on reduced transport models in ASTRA [3,4]. Figure 5 shows the predictive temperature profiles in the flattop phase.



#### 2.4.2 High-performance steady-state scenario

Various 0.5D and 1.5D integrated modelling codes have been applied to develop and optimize the high-performance steady-state scenario in the physics design of EHL-2. By taking into account 10 MW of 80 keV tangential NBI (tangency radius R=0.8 m) and 5 MW of ECRH current drive (deposition location set to  $\rho=0.4$  m), a high-performance plasma with a large bootstrap current component ( $f_{bs}>50\%$ ) can be established with a range of Ip between 1.0 and 1.5 MA, as shown in figure 6.



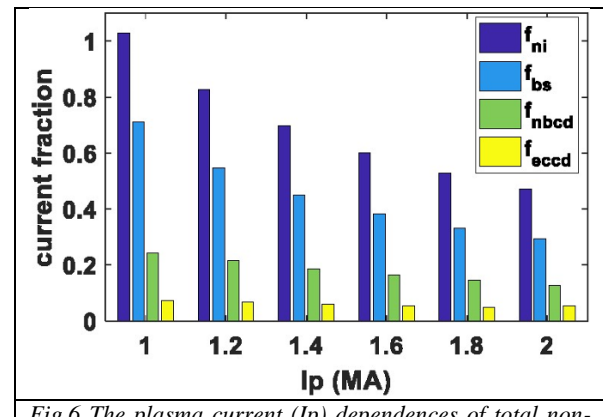


Fig.6 The plasma current (Ip) dependences of total noninductive current fraction ( $f_{ni}$ ), the bootstrap current fraction ( $f_{bs}$ ), the current fractions driven by NBI ( $f_{nbcd}$ ), and the current fraction driven by ECRH ( $f_{eccd}$ )[2].

A comparison of EHL-2 plasma ion temperature and triple products simulated by ASTRA with different values of Ip,  $B_t$  and  $n_e$ , as shown in figure 2. Comparison of plasma radial profiles between two plasmas with 2 T/2 MA and 2.5 T/2.5 MA of magnetic field/plasma current is shown in Fig. 7.

#### 3. PHYSICS DESIGN: KEY PHYSICS ISSUES

#### 3.1 Start-up and non-inductive current drive

In order to achieve the current flat-top in the limit time, the plasma current ramp-up rate on EHL-2 needs to reach 3–5 MA/s, which makes the current drive in EHL-2 more challenging. Therefore, non-inductive current drive must play a key role in EHL-2. To this end, we have developed a strategy to achieve current drive required for the EHL-2 design. (1) The start-up phase will be realized with fully noninductive mode with ECRH. (2) The ramp-up phase will be accomplished with the synergetic mode between ECRH, CS, NBI, and LHCD.

#### 3.2 Effects of boron on the plasma transport

We performed first-principles-based simulations using the gyro-kinetic code GENE [5, 6] to simulate the turbulent transport characteristics of hydrogen-boron plasmas with boron fractions ranging from 0 to approximately 15%, as shown in Fig. 8. This finding confirms the reliability of the current EHL-2 design and provides an innovative perspective for the fuel design for steady-state operation of future fusion reactors.

# 3.3 H-mode access and pedestal stability

Based on the experimental scaling law for STs [7], the L-H transition threshold power is expected to be in the range of 25 MW, which is about one-third of the plasma absorption power. This indicates that the main operating scenarios of the EHL-2 physics design will all operate in the H-mode regime [8], which also means that the physics design needs to face the challenge of ELM control [9]. Furthermore, the pedestal structure, which determined by the constraints of peeling-ballooning modes (PBM) and kinetic ballooning modes (KBM), has been calculated using the REPED model [10,11] as shown in figure 9. The preliminary results indicate that the pedestal heights are lower in the high-ion temperature scenario ( $T_i/T_e > 1$ ;  $T_{i,0}$  exceeds 25 keV) compared to the thermal equilibrium case  $(T_i/T_e = 1; T_{i,0} = 15)$ keV).

An in-vessel resonant magnetic perturbation (RMP) coil system has been preliminarily designed for ELM control on EHL-2. the physics design of this coil system will focus

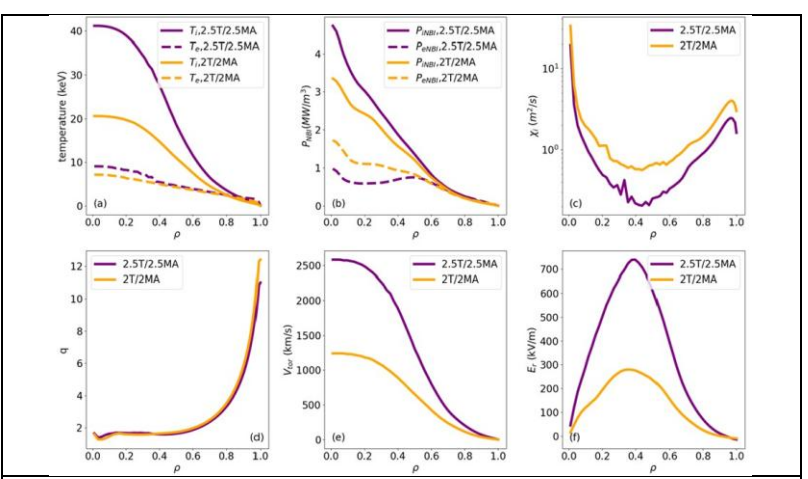


Fig. 7 Comparison of plasma radial profiles. The simulation cases correspond to the ones in figures 2 and 5[2].

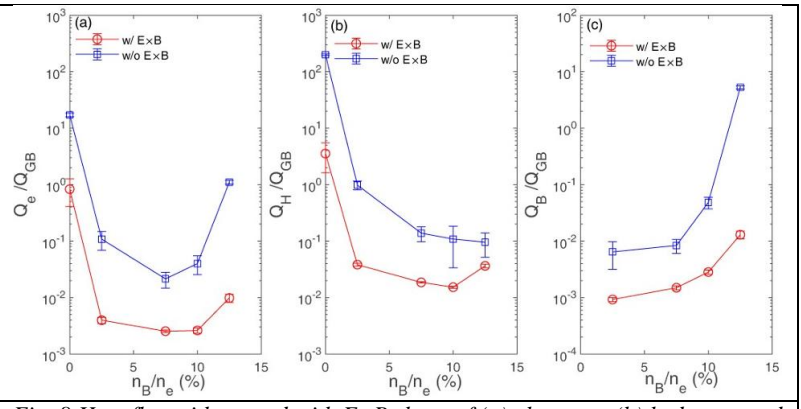


Fig. 8 Heat flux without and with  $E \times B$  shear of (a) electrons, (b) hydrogen and (c) boron under boron fraction scan[2].

on generating RMPs with low toroidal mode number ( $n \le 2$ ) and high poloidal mode number ( $m \ge 5$ ) [12,13].

#### 3.4 MHD stability and control

To avoid disruption caused by VDE, we have conducted an analysis of the passive stabilizing plate (PSP), which can help optimize engineering design. In addition, a pair of in-vessel fast control coils will be designed to provide feedback control of the VDE on EHL-2. The future high-power heated EHL-2 plasma is basically operated in an H-mode regime, and the plasma poloidal beta is higher than the beta threshold of the neoclassical tearing mode (NTM).

#### 3.5 Analysis of fast ion losses

For beam ions, the calculation indicates that the losses are generally minimal under standard operating

conditions. With a magnetic field B<sub>t</sub> of 2 T and plasma current Ip of 1.5 MA, the loss fraction is less than 1%. However, when Ip drops to 500 kA, the loss fraction for 200 keV beam ions increases dramatically to 32%, underscoring the importance of maintaining appropriate plasma parameters for effective particle confinement.

Alpha particle losses exhibit higher loss fraction even under enhanced operational parameters. With a magnetic field of 3 T and plasma current of 3 MA, the lost fractions are 3.86% for thermal reaction products and 18.86% for beam-target reaction products, corresponding to fusion powers of 290 W and 1271 W, respectively. As shown in the figure 10, these losses occur predominantly at the outer moving limiter, with a smaller portion at the upper divertor plates. The toroidal distribution of alpha particle losses is nearly uniform, showing no preferential directional tendency.

The ripple amplitude at the plasma closed flux surface is less than 0.01%. Consequently, the ripple field effect on particle loss is negligible.

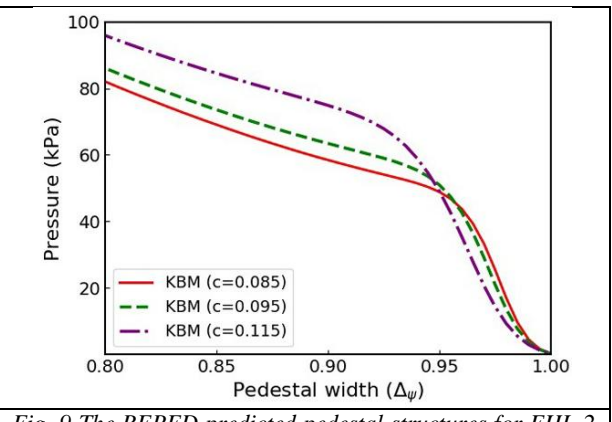


Fig. 9 The REPED predicted pedestal structures for EHL-2 H-mode H-B plasmas[2].

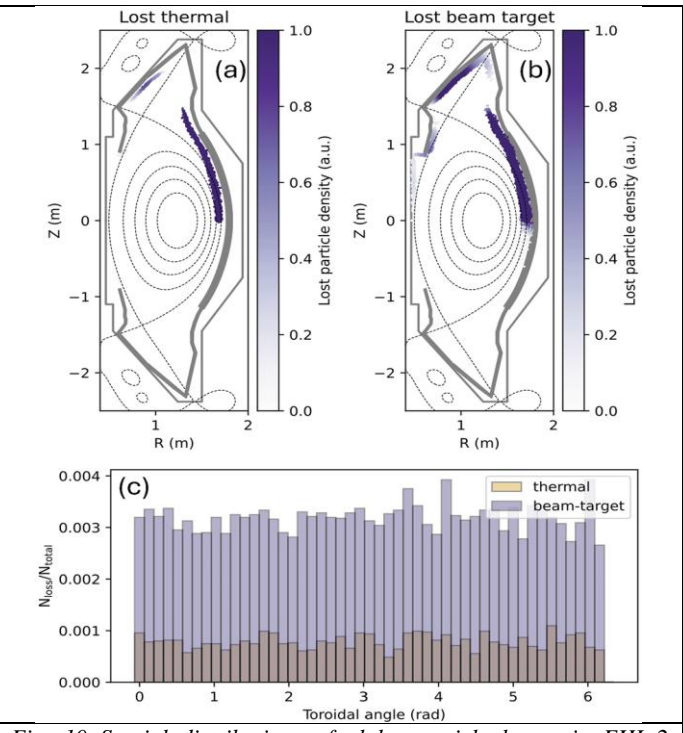


Fig. 10 Spatial distributions of alpha particle losses in EHL-2 tokamak[2].

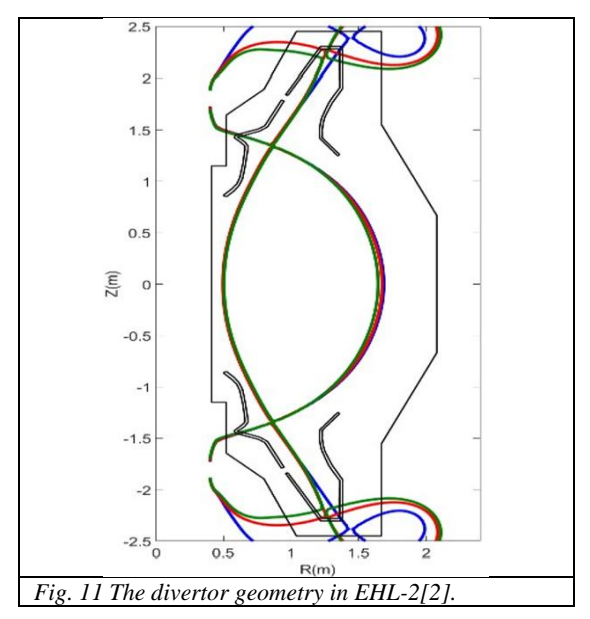
#### 3.6 Power and particle handling

In order to control the heat flux density and electron temperature at the targets in EHL-2 with high heat power, a new initiative has been launched on EHL-2 to develop a closed divertor for evaluating boundary plasma solutions applicable to the next step fusion experiments, as shown in figure 11 [14].

To quantify the onset of detachment, a systematic scan of the separatrix density,  $n_{e,sep}$ , at the outer middle-plane, is carried out. In figure 12 the peak values for electron temperature, perpendicular heat flux density and parallel particle flux density at the inner and outer targets are plotted as a function of  $n_{e,sep}$ .

The peak values for electron temperature at the inner target and outer target can be reduced to  $10\,\text{eV}$  respectively, when  $n_{\text{e,sep}}$  is increased to  $1.66\times10^{19}\,\text{m}^{-3}$ . The corresponding peak values of perpendicular heat flux density for the inner and outer targets are reduced to  $1\,\text{MW/m}^2$  and  $0.2\,\text{MW/m}^2$  respectively. The rollover of parallel particle flux density is usually used as an indicator for the onset of detachment, so the inner and outer divertor target enter detachment with the lower upstream separatrix density  $1.75\times10^{19}\,\text{m}^{-3}$ .

# 3.7 Disruption prediction and mitigation strategies



Effective disruption mitigation relies on the ability to predict disruptions in advance. The data-driven neural networks have been employed for disruption prediction on EXL-50 [15] and EXL-50U tokamak [16], which were used to validate the design of EHL-2. The accuracy and responsiveness of the neural networks have been confirmed.

In EHL-2, it is challenging for the injected gas to reach deeper plasma with high pressure gradients, for that reason shattered SPI (shattered pellet injection) is the main candidate designed for disruption mitigation in EHL-2.

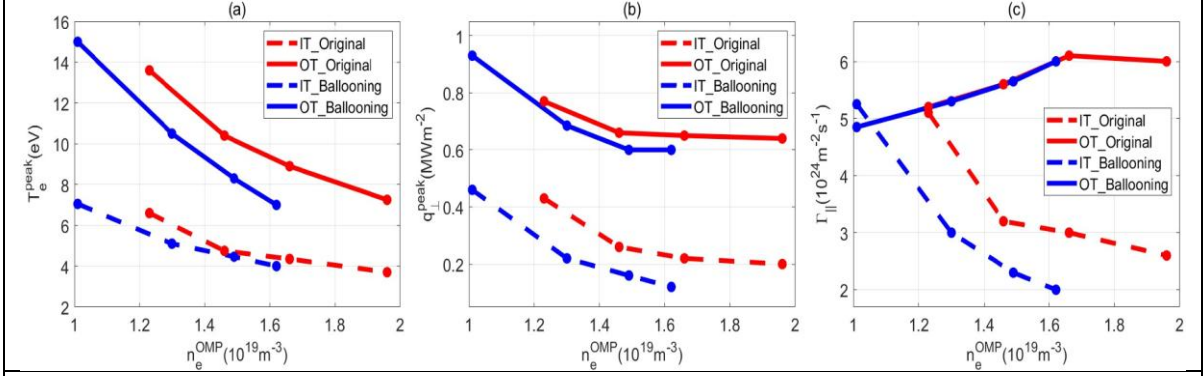


Fig. 12 Peak values of (a) electron temperature, (b) perpendicular heat flux density and (c) parallel particle flux density at the inner and outer targets as a function of the upstream separatrix density[2].

# 3.8 Challenges of p-11B fusion alpha particle power conversion

In the EHL-2 design, we have identified four major challenges in energy conversion for ST p-<sup>11</sup>B fusion that must be addressed in an integrated manner: (1) aligning and directing the charged particles for efficient extraction; (2) recovering the energy from the extracted charged particles; (3) recovering radiation energy and other forms of energy that cannot be directly converted into electricity; and (4) understanding the characteristics of charged particle losses and extraction within the electromagnetic field structure inherent to the ST. While we have conducted preliminary studies on challenges (2) and (4), these efforts are still insufficient to develop a viable solution for a p-11B reactor [17], highlighting the need for further research to overcome these challenges.

#### 4. EHL-2 EXPERIMENTAL STRATEGY

Table 3. Experimental strategy of EHL-2[2]

14010 3. 1	EHL-2 Experimental Strategy			Diverto	NBI (keV/5s)		ECRH (GHz/5s)		ICRH (MHz/ 5s)	LHW (GHz/ 5s)	Total heating	
	Phase	Estimated Time	Goal	'	60	80-100	200	50	105&140	30-75	2.45-5	power
y1)	I	3 m	Engineering test: toroidal field/control/ diagnostics, etc. Physics test: ECRH startup  1 MA operation					1 MW	3 MW			4 MW
				(1 m) Mai	Maintenance/Upgrade							
		3 m	•2 MA/2 T	slab	4 MW							
	II		Achieve long-leg divertor configuration					1 MW	4 MW			9 MW
			•Ti > 3 keV, Ti/Te >2 (NBI heating validation)									
	(1 m) Maintenance/Upgrade											
	Ш	3 m	High-ion-temperature scenario validation: Ti > 10 keV, Ti/Te >2		4 MW	5 MW		1 MW	6 MW			16 MW
			(2 m)	Maintenan	ce/Upgra	ade						
Integrated Research (2 yr)	I	10 m	•Ti > 25 keV, Ti/Te >2 •H–B thermonuclear reaction validation •High-performance scenario validation: fully non-inductive current drive	closed	4 MW	10 MW	3 MW	1 MW	6 MW			24 MW
				(2 m) Maintenance/Upgrade								
	П	8 m	•ICRH–NBI synergy validation		4 MW	10 MW	3 MW	1 MW	6 MW	2 MW		26 MW
			(2 m)	Maintenan	ce/Upgra	ade						
Extended Research (>1 yr)			•3 MA; 3T •Ti > 35 keV, Ti/Te >2 •High triple-product scenario development, ST scaling law validation •H–B fusion gain validation		4 MW	10 MW	3 MW	1 MW	6 MW	5 MW	2 MW	31 MW

The experimental strategy of EHL-2 is shown in Table 3. On the first phase of initial research, we will aim at engineering test, physics test (ECRH startup) and 1 MA operation with 4MW ECRH in limiter configuration. The goals are achieving 2 MA/2 T, long-leg divertor configuration and Ti>3 keV with Ti/Te>2 on the second phase with the total heating power of 9 MW. On the third phase, we will focus on the validation of high-ion-temperature scenario (Ti>10 keV with Ti/Te>2) with the total heating power of 16 MW.

After the three phases of initial research, it comes to integrated research for EHL-2. The integrated research consists with 2 phases. On the first phase (with 24 MW total heating power and closed divertor), our goals are (1) achieve Ti>25 keV with Ti/Te>2; (2) H-B thermonuclear reaction validation; (3) high-performance scenario validation: fully non-inductive current drive. On the second phase, ICRH-NBI synergy validation will be studied. Then, we will pursue extended research (with the total heating power of 31 MW) such as 3 MA/3 T, Ti>35 keV with Ti/Te>2, high triple-product scenario development, ST scaling law validation and H-B fusion gain validation.

#### REFERENCES

- [1] M. S. Liu, H. S. Xie, Y. M. Wang, Phys. Plasmas 31, 062507 (2024).
- [2] Y. F. Liang, H. S. Xie, Y. J. Shi et al, Plasma Science and Technology, 27, 2, 024001 (2025).
- [3] Pereverzev G and Yushmanov P N, IPP-Report IPP-598 Garching: Max-Planck-Institut fuer Plasmaphysik (2002)
- [4] Wang X Y et al 2025 Plasma Sci. Technol. 27 024007(2025).
- [5] Görler T et al, J. Comput. Phys. 230 7053 (2011)
- [6] Tan M Z et al, Plasma Phys. Control. Fusion 67 025018 (2025)
- [7] Kurskiev G S et al, Nucl. Fusion 62 016011 (2022)
- [8] Wagner F et al, Phys. Rev. Lett. 49 1408 (1982)
- [9] Liang Y, Fusion Sci. Technol. 59 586 (2011)
- [10] Li K et al, Nucl. Fusion 61 096002 (2021)
- [11] Wang Y M et al, Plasma Sci. Technol. 27 024005 (2025)
- [12] Liang Y et al, Phys. Rev. Lett. 98 265004 (2007)
- [13] Liang Y et al, Phys. Rev. Lett. 105 065001 (2010)
- [14] Wang F Q et al, Plasma Sci. Technol. 27 024009 (2025)
- [15] Cai J Q et al, Plasma Sci. Technol. 26 055102 (2024)
- [16] Cai J Q et al, Plasma Sci. Technol. 27 024013 (2025)
- [17] Xie H S et al, Plasma Sci. Technol. 27 024010 (2025)